

Spread of dendritic excitation in layer 2/3 pyramidal neurons in rat barrel cortex *in vivo*

Karel Svoboda^{1,2}, Fritjof Helmchen², Winfried Denk² and David W. Tank²

¹ Cold Spring Harbor Laboratory, Cold Spring Harbor, New York 11724, USA

² Biological Computation Research Department, Bell Laboratories, Lucent Technologies, 600 Mountain Avenue, Murray Hill, New Jersey 07974, USA

Correspondence should be addressed to K.S. (svoboda@cshl.org)

In layer 2/3 pyramidal neurons of barrel cortex *in vivo*, calcium ion concentration ($[Ca^{2+}]$) transients in apical dendrites evoked by sodium action potentials are limited to regions close to the soma. To study the mechanisms underlying this restricted pattern of calcium influx, we combined two-photon imaging of dendritic $[Ca^{2+}]$ dynamics with dendritic membrane potential measurements. We found that sodium action potentials attenuated and broadened rapidly with distance from the soma. However, dendrites of layer 2/3 cells were electrically excitable, and direct current injections could evoke large $[Ca^{2+}]$ transients. The restricted pattern of dendritic $[Ca^{2+}]$ transients is therefore due to a failure of sodium action-potential propagation into dendrites. Also, stimulating subcortical activating systems by tail pinch can enhance dendritic $[Ca^{2+}]$ influx induced by a sensory stimulus by increasing cellular excitability, consistent with the importance of these systems in plasticity and learning.

Sodium action potentials can propagate somatofugally into the dendritic tree of cortical pyramidal neurons¹, as shown by electrophysiology and optical imaging of $[Ca^{2+}]$ in brain slices (for reviews, see ref. 2). Because action potentials open voltage-sensitive calcium channels (VSCCs)^{3,4} and relieve the magnesium block of NMDA receptors⁵, they could be important in long-term synaptic plasticity. Consistent with this notion, synaptic activity coincident with back-propagating sodium action potentials induces some types of long-term potentiation (LTP) in hippocampus⁶ and neocortex⁷. Strong synaptic stimulation can evoke forward-propagating sodium action potentials⁸ and dendritic calcium spikes^{3,10,11} in pyramidal cell dendrites, both of which could serve to amplify distal synaptic currents⁹.

However, dendritic excitability depends on factors that are difficult to reproduce *in vitro*. For example, dendritic excitability is enhanced by cholinergic modulation¹² and probably other modulatory systems and is suppressed by inhibitory inputs^{13,14}. Dendritic excitability is also strongly affected by ionic composition¹⁵ and by the activity-dependent activation and inactivation of voltage-sensitive conductances^{16–18}. Also, unlike *in vivo*, neurons in a slice are silent; synaptic ‘chatter’ therefore does not modulate their integrative properties. Measurements confirm that dendritic electrophysiology may differ *in vivo* compared to slices. Membrane leak in pyramidal neurons of cat neocortex is dominated by background synaptic activity¹⁹ that could restrict the spread of dendritic excitability²⁰. Similarly, depending on the state of the hippocampal network, sodium action potentials generated in dendrites of CA1 pyramidal neurons may not propagate into the soma²¹.

We applied two-photon excitation laser scanning microscopy²² (2PLSM) to dendritic $[Ca^{2+}]$ imaging in the intact brain^{23,24}. $[Ca^{2+}]$ imaging quantifies excitation in parts of the dendritic tree inaccessible to electrodes and in different regions in the same cell and helps disambiguate the biophysical basis of electrical events, such as calcium spikes and large postsynaptic potentials. In addition, $[Ca^{2+}]$

itself controls neuronal dynamics. In the dendrites of layer 2/3 pyramidal neurons, whisker stimulation produced fast-rising $[Ca^{2+}]$ transients only coincident with sodium action potentials²³. The amplitudes of $[Ca^{2+}]$ transients were proportional to the number of sodium action potentials in a short burst, indicating that dendritic $[Ca^{2+}]$ may encode the neuron’s recent activity²⁵. The spatial pattern of calcium influx evoked by sodium action potentials peaked in the proximal apical dendrite and declined steeply with increasing distance from the soma, with no detectable $[Ca^{2+}]$ rise in the distal branches, suggesting that backpropagation of sodium action potentials could be highly restricted *in vivo*. Sodium action potentials therefore may not produce sufficient depolarization in distal dendrites to unblock NMDA receptors⁵ or open VSCCs⁴.

Agonists of muscarinic acetylcholine receptors can enhance dendritic electrogenesis^{12,26}. Dendrites of barrel-cortex pyramidal neurons contain these receptors²⁷, suggesting that neuromodulation could control dendritic excitation *in vivo*. In the intact animal, activity in the cholinergic basal forebrain (nucleus basalis) correlates with active exploratory behavior, as opposed to rest²⁸, and activity in this system modulates learning and memory²⁹. In anesthetized animals, tail pinch activates the neocortex³⁰, at least in part due to activation of nucleus basalis³¹.

Here we combined somatic or dendritic membrane potential measurements with dendritic $[Ca^{2+}]$ imaging to study mechanisms underlying the spatial pattern of action potential-evoked calcium influx. We then tested if calcium action potentials can be evoked *in vivo* and explored the effects of cortical activation by tail pinch.

Results

INTRACELLULAR RECORDING COMBINED WITH 2PLSM IMAGING

Anesthetized rats were surgically prepared for electrophysiology and imaging (Fig. 1a). Sharp micropipettes were used to record the membrane potential of regular-spiking³³ pyramidal

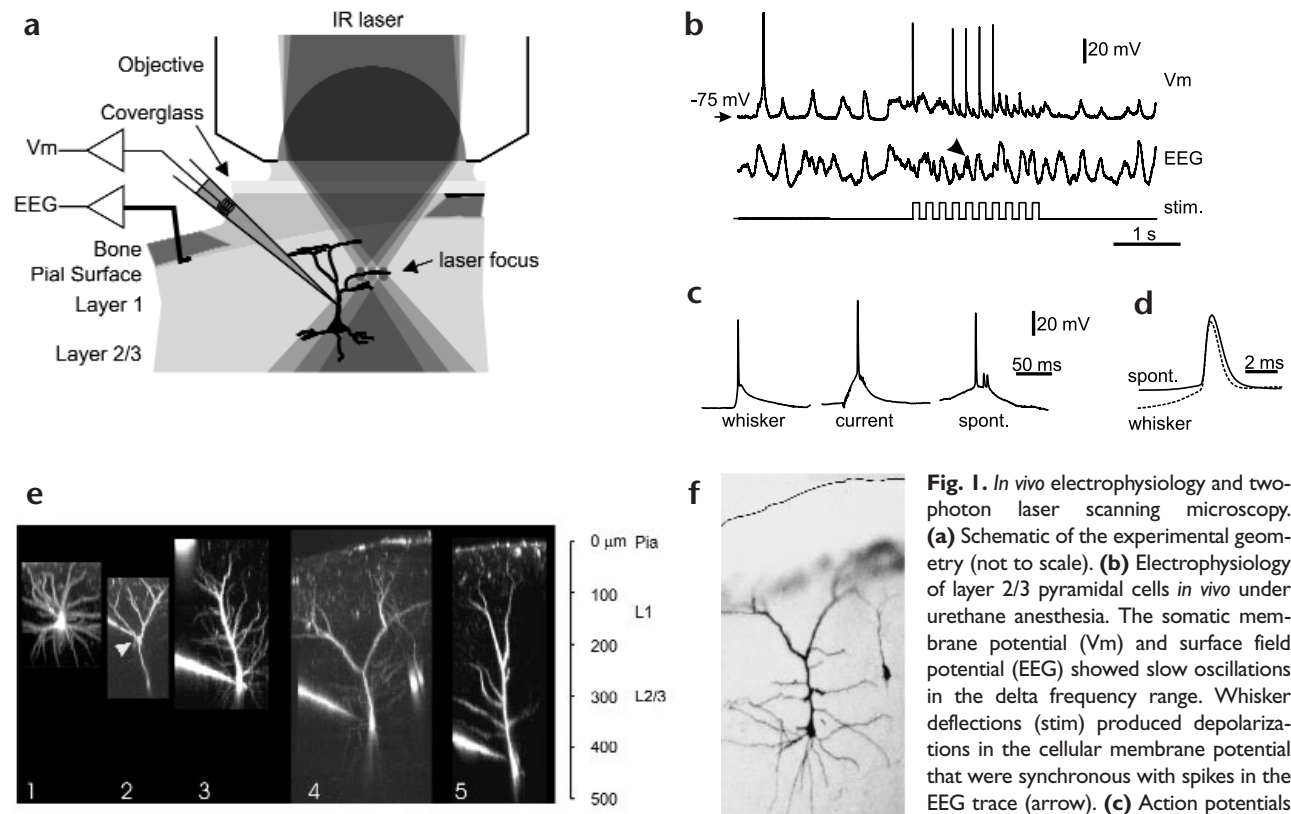


Fig. 1. *In vivo* electrophysiology and two-photon laser scanning microscopy. **(a)** Schematic of the experimental geometry (not to scale). **(b)** Electrophysiology of layer 2/3 pyramidal cells *in vivo* under urethane anesthesia. The somatic membrane potential (V_m) and surface field potential (EEG) showed slow oscillations in the delta frequency range. Whisker deflections (stim.) produced depolarizations in the cellular membrane potential that were synchronous with spikes in the EEG trace (arrow). **(c)** Action potentials evoked by whisker deflection (left, average of 15 trials), current injection (middle, 12 trials) or spontaneous synaptic potentials (right, 4 trials; small spikes to the right of the action potential are averaging artifacts). **(d)** Enlargement of spontaneous (solid line) and whisker-evoked (dashed line) action potentials. **(e)** Representative diverse morphologies of layer 2/3 pyramidal cells based on 2PLSM images. The reconstructions are maximum-value projections of stacks of images acquired with 0.5–2 μm spacing. Penetration sites were somatic (1, 3–5) or dendritic (2, arrow); one morphology was acquired after electrode withdrawal (1). **(f)** Layer 2/3 neuron stained with neurobiotin and visualized with peroxidase-DAB reaction. Same cell as panel 4 in (e).

age of 15 trials), current injection (middle, 12 trials) or spontaneous synaptic potentials (right, 4 trials; small spikes to the right of the action potential are averaging artifacts). **(d)** Enlargement of spontaneous (solid line) and whisker-evoked (dashed line) action potentials. **(e)** Representative diverse morphologies of layer 2/3 pyramidal cells based on 2PLSM images. The reconstructions are maximum-value projections of stacks of images acquired with 0.5–2 μm spacing. Penetration sites were somatic (1, 3–5) or dendritic (2, arrow); one morphology was acquired after electrode withdrawal (1). **(f)** Layer 2/3 neuron stained with neurobiotin and visualized with peroxidase-DAB reaction. Same cell as panel 4 in (e).

cells in layer 2/3 of primary somatosensory cortex ($n = 114$). Apparent resting membrane potentials were -60 to -85 mV, and spontaneous somatic action potential amplitudes were larger than 50 mV (78 ± 7 mV, mean \pm standard deviation, $n = 10$) and narrower than 1.5 ms (width at half maximal amplitude, 1.24 ± 0.12 ms, $n = 10$). Apparent cellular input resistance averaged 46 ± 12 M Ω ($n = 20$). Membrane potentials showed pronounced spontaneous fluctuations (amplitude ~ 10 –20 mV; frequency ~ 1 –4 Hz)³⁴ and some background spiking (0–10 Hz)¹⁹ (Fig. 1b). Electroencephalograph (EEG) potentials were recorded epidurally at the lateral edge of barrel cortex (Fig. 1a). Spontaneous membrane potential fluctuations were highly correlated with the EEG potential, suggesting that the cortical background activity is highly synchronous³⁵ (Figs. 1b, 2a and 3a). Trains of whisker deflections (5 Hz, 2 s) produced ~ 20 mV depolarizations lasting ~ 10 –20 ms that often were accompanied by a brief burst of action potentials (up to three action potentials per burst)²³ (Figs. 1b, c and 2a). Whisker deflections also produced spikes in the cortical EEG signal (width 10–20 ms), revealing additional synchronized cortical activation in response to whisker deflection (Figs. 1b, 2a, 3a and 6a). EEG spikes were not evoked with every cycle of whisker deflection, but had characteristics of all-or-nothing events, suggesting a highly nonlinear process³⁶ (Figs. 1b, 2a and 6a). Action potentials evoked by whisker deflection were smaller (by $10 \pm 3\%$) and narrower (by $15 \pm 6\%$, $n = 5$) than those pro-

duced by spontaneous postsynaptic potentials (PSPs) (Fig. 1c and d). Action potentials evoked by current injection were at least as large as those evoked by PSPs (Fig. 1c), but systematic bridge-balance errors may have perturbed these measurements.

Microelectrodes were also used to load neurons iontophoretically with a $[\text{Ca}^{2+}]$ -sensitive fluorophore (Oregon Green Bapta 1 or Calcium Green 1; Fig. 1a). Several minutes of dye loading often sufficed to label neurons throughout most of the dendritic tree. Unless obstructed by large blood vessels, a complete picture of the dendritic morphology could be acquired (Fig. 1e). Pyramidal neurons were morphologically diverse; superficial cells (depth of soma < 250 μm) had no pronounced apical trunk, whereas deeper cells (depth of soma 200–500 μm) fit the standard description of pyramidal cells, dominated by an apical dendrite (Fig. 1e and f). All neurons in this study were spiny and presumably excitatory³⁷. In four experiments, neurobiotin was included in the recording pipette for *postmortem* histology. Cellular morphologies reconstructed from *in vivo* 2PLSM and fixed-tissue bright-field microscopy were similar (Fig. 1e and f).

We used 2PLSM to identify the location of the recording electrode, which was possible within minutes after establishing intracellular recording conditions, because this allowed selection for dendritic recordings (Figs. 1e and 5a). Approximately 20% ($n = 25$) of our penetrations were dendritic, located mostly on the main apical shaft, 20–200 μm from the soma.

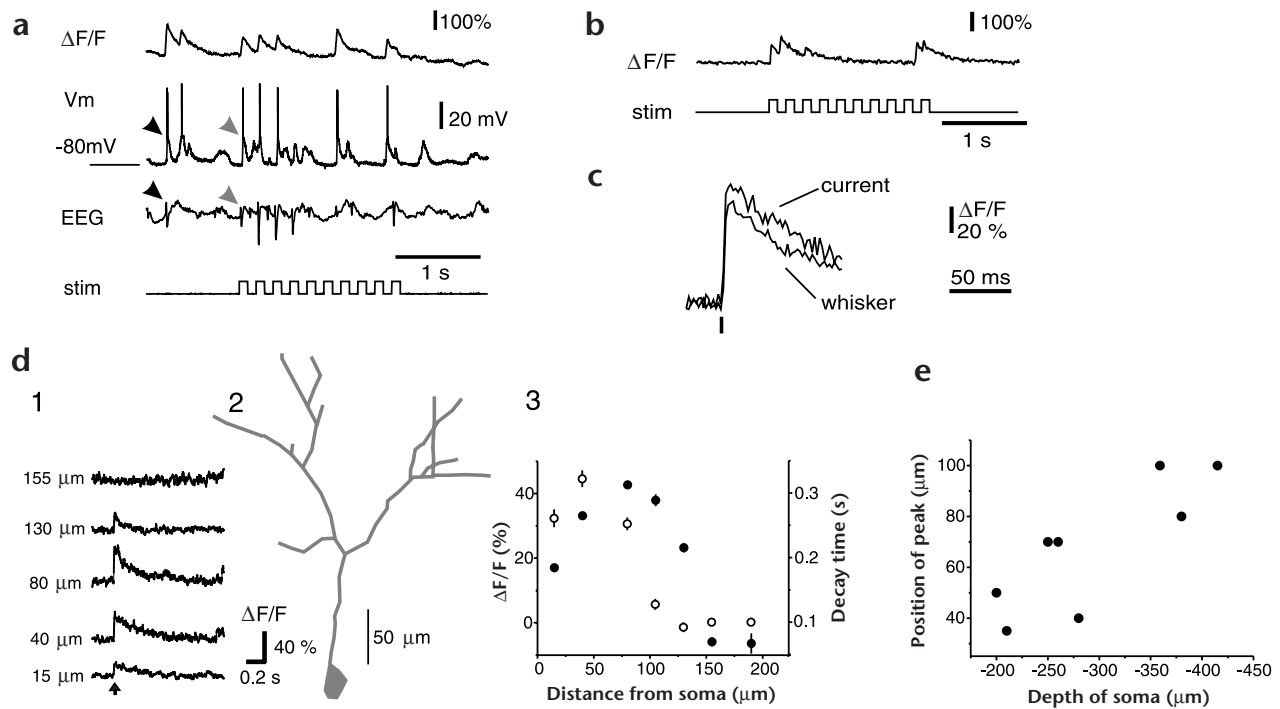


Fig. 2. Dendritic $[Ca^{2+}]$ transients evoked by sodium action potentials. **(a)** Dendritic $[Ca^{2+}]$ transients ($\Delta F/F$), somatic membrane potential (V_m) and network activity (EEG) in response to whisker deflection (stim). The soma was $290\ \mu\text{m}$ below the surface of the brain; $[Ca^{2+}]$ transients were measured $70\ \mu\text{m}$ above the soma. The neuron produced spontaneous (V_m , black arrow) and whisker-deflection-evoked (V_m , gray arrow) action potentials. During the stimulus train, the EEG trace showed pronounced downward deflections (EEG, gray arrow) that were synchronized with slow membrane depolarizations. These depolarizations produced action potentials, which in turn caused dendritic $[Ca^{2+}]$ influx. **(b)** Whisker-stimulation-evoked $[Ca^{2+}]$ transients two hours after electrode removal. **(c)** Comparison of $[Ca^{2+}]$ transients associated with single action potentials (arrow) evoked by somatic current injection (dashed line) or whisker deflection (solid line). (Traces are averages of 10 trials.) **(d)** Spatial map of dendritic $[Ca^{2+}]$ transients. Single sodium action potentials (1, arrow) were evoked by current injection. The resulting $[Ca^{2+}]$ -transient amplitudes varied with the distance from the soma. (Traces are averages of 4 trials.) 2, Neuronal morphology (same neuron as in Fig. 1e, panel 4 and f). 3, $[Ca^{2+}]$ transient amplitudes (solid circles) and decay times (open circles) as a function of height above the soma. **(e)** Distance between soma and peaks of the spatial maps of dendritic $[Ca^{2+}]$ transients as a function of soma depth.

ACTION-POTENTIAL-EVOKED DENDRITIC $[Ca^{2+}]$ TRANSIENTS
 2PLSM imaging was also used for rapid measurements (time resolution $\sim 2\ \text{ms}$) of dendritic $[Ca^{2+}]$ dynamics using the line-scan mode (displayed as fractional changes in fluorescence, $\Delta F/F$; Fig. 2a). Whisker stimulation (Fig. 2a and b), spontaneous PSPs (Fig. 2a) and somatic current injections through the recording electrodes (Fig. 2d, panel 1) all evoked large $[Ca^{2+}]$ transients ($\Delta F/F$ up to 400%) in the proximal dendrites. Dendritic $[Ca^{2+}]$ transients under these conditions were always associated with somatically recorded sodium action potentials (Figs 2a, c and d, 4 and 6), rising rapidly (within 2 ms) after the action potential. The magnitudes of dendritic $[Ca^{2+}]$ transients evoked by whisker deflection were similar after electrode withdrawal, suggesting that the presence of the recording electrode did not significantly perturb neuronal electrogenesis (Fig. 2b). $[Ca^{2+}]$ transients associated with action potentials evoked with whisker deflection were smaller (by $17 \pm 8\%$, $n = 5$) than those evoked by current injection (Fig. 2c), probably reflecting the difference in action-potential amplitudes and durations (Fig. 1c and d).

$[Ca^{2+}]$ transients associated with sodium action potentials were limited to the proximal dendrites and were undetectable in the distal tuft branches of layer 1 (ref. 23; Fig. 2d). Transients in the somata were small, possibly because of the unfavorable surface-to-volume ratios or because of the short duration of the

somatic action potential. In deep cells with long apical dendrites, the peak of calcium influx appeared farther from the soma than in shallower cells with short dendrites (Fig. 2e).

DENDRITIC SODIUM ACTION POTENTIALS

To investigate the mechanisms underlying these spatial maps of $[Ca^{2+}]$ transients, we measured action-potential amplitudes and shapes in dendrites. Dendritic membrane potential measurements (Fig. 3) were stable for up to one hour. Because dendritic diameters are small, electrode leak and potassium loading produced by the electrode penetration could alter excitability. To avoid overloading neurons with potassium, we used only 400 mM potassium acetate. We also did several control experiments. First, $[Ca^{2+}]$ transients produced by current injection were measured in the vicinity of the electrode penetration. These experiments showed that fluorescence transients can be large ($> 100\%$) even close to the penetration site, and therefore resting $[Ca^{2+}]$ levels must be low (less than the calcium binding affinity for the indicator, $\sim 170\ \text{nM}$, $n = 10$; Fig. 5). Second, the spatial maps of $[Ca^{2+}]$ transients were similar in dendritic and somatic penetrations and in cells where the electrode had been withdrawn²³. Our experiments suggest that membrane leak and potassium loading from the electrode penetration do not produce high resting $[Ca^{2+}]$ levels or otherwise severely perturb dendritic electrogenesis, although we cannot exclude subtle effects.

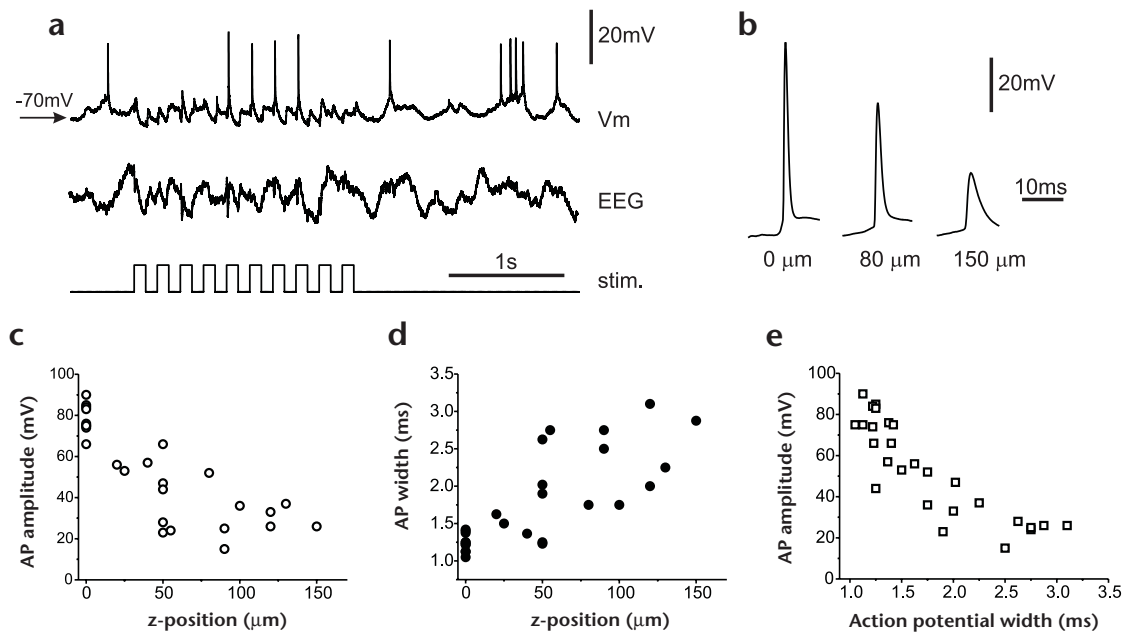


Fig. 3. Properties of dendritic sodium action potentials. **(a)** Dendritic membrane potential measurement (V_m) in the apical dendrite of a pyramidal cell, 150 μm above the soma. The soma was 250 μm deep. **(b)** Representative averaged action potential shapes. Left, somatic; middle, 80 μm above the soma; right, 150 μm above the soma. Fifteen spontaneous action potentials were averaged for each trace. **(c)** Amplitudes of action potentials (AP) generated by spontaneous postsynaptic potentials (average of 10–15 traces each) as a function of distance from soma. Amplitude was defined as the difference between the peak amplitude and baseline 100 ms before the peak. **(d)** Action potential width as a function of distance from soma. Widths were measured at half-maximum from averaged action potentials. **(e)** Action-potential amplitude as a function of action-potential width, showing a strong correlation.

Dendritic resting potentials (range -60 to -85 mV) and input resistances (49 ± 13 M Ω , $n = 10$) were indistinguishable from those in the soma. Dendritic membrane potentials fluctuated in synchrony with the EEG trace, and whisker deflection produced sharp spikes in the EEG that were accompanied by PSPs and action potentials in the dendritic membrane potential (Fig. 3a). However, average sodium action potential amplitudes decreased rapidly with distance from the soma (Fig. 3b and c). Similarly, average action potential widths increased with distance from the soma (Fig. 3b and d). Action potential widths and amplitudes were highly correlated (Fig. 3e). Our measurements of sodium action potential amplitudes are similar to results from CA1 (ref. 6) and layer 5 pyramidal cells³⁸ *in vitro* and CA1 pyramidal cells *in vivo*²¹. However, compared to these measurements, action potential amplitudes in layer 2/3 neurons *in vivo* decreased more rapidly with distance from the soma (Fig. 3c), to only ~ 25 mV about 150 μm above the soma. Such dendritic action potential amplitudes and widths are consistent with passive spread of sodium action potentials into dendrites^{39,40}. Our observation of decremental action potential spread into the dendrites of layer 2/3 pyramidal cells explains the lack of $[\text{Ca}^{2+}]$ transients in distal den-

$[\text{Ca}^{2+}]$ TRANSIENTS DUE TO SODIUM ACTION POTENTIAL BURSTS

Brain slice experiments have suggested that sodium action potentials show activity-dependent propagation into dendrites^{38,41,42}. The first action potential in a burst is thought to propagate throughout a large part of the dendritic tree, whereas later action potentials attenuate more rapidly with distance from the soma. Thus, the amplitudes of action-potential-evoked $[\text{Ca}^{2+}]$ transients decrease with time in a burst, especially in distal den-

drites^{41,42}. This activity-dependent attenuation of backpropagation has been interpreted to mean that later action potentials in a burst fail to propagate actively into dendrites⁴², but if the first action potential fails, as we suspect occurs for layer 2/3 cells *in vivo*, this activity-dependent inactivation should not be observed.

To test this notion, brief bursts of action potentials (interspike intervals ~ 6 –8 ms) were evoked with somatic current injections (1–4 spikes; longer bursts produced $[\text{Ca}^{2+}]$ transients that exceeded the linear range of the $[\text{Ca}^{2+}]$ indicator) or whisker deflections (1–2 spikes) (Fig. 4). $[\text{Ca}^{2+}]$ transients associated with sensory stimulation or current-injection-evoked action potentials were measured at various distances along the apical dendrites of several pyramidal cells. $[\text{Ca}^{2+}]$ transient amplitudes always scaled approximately linearly with action potential number (Fig. 4). This lack of activity-dependent attenuation of $[\text{Ca}^{2+}]$ transients was also seen at longer interspike intervals (for example, see the whisker-deflection-evoked transients at 5 Hz in Fig. 2a)²³. Direct measurements of dendritic action-potential amplitudes also failed to show activity-dependent attenuation (Figs 3a and 6c). Thus it seems that the activity-dependent decrement in dendritic action-potential amplitudes observed in brain slices is reduced in layer 2/3 pyramidal neurons in our preparation *in vivo*. This observation is consistent with our dendritic membrane-potential measurements, which suggest that even the first action potential in a burst fails to backpropagate into the dendrites.

DENDRITIC CALCIUM SPIKES

We previously showed that sensory activation of layer 2/3 neurons does not produce dendritic calcium spikes in this preparation²³. However, dendrites of neocortical^{10,11} and hippocampal¹⁵

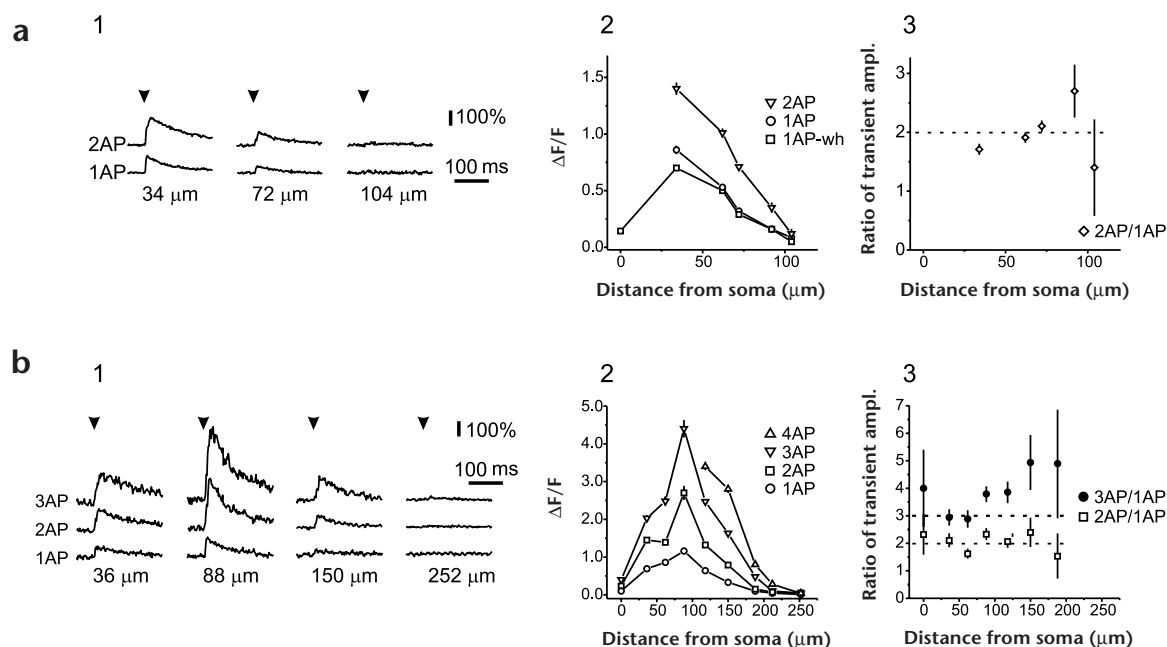


Fig. 4. Dendritic $[Ca^{2+}]$ transients evoked by sodium action potential bursts. **(a)** Superficial pyramidal cell (soma was 210 μm below the surface of the brain). 1, Averaged $[Ca^{2+}]$ transients in response to one (1AP) or two (2AP) sodium action potentials (arrows) evoked by current injection measured at various heights above the soma (averages of 10–15 trials each). Interspike intervals within a burst were 6–8 ms. 2, Map of $[Ca^{2+}]$ transients along the apical dendrite. Transients were evoked by current injection (1AP, 2AP) or whisker deflection (1AP-wh). Note that smaller transients were evoked by whisker deflection than by current injection. 3, Amplitudes of $[Ca^{2+}]$ transients evoked by two action potentials, normalized to transients evoked by one action potential. **(b)** Moderately deep layer 2/3 pyramidal neuron (soma was 360 μm below the surface of the brain). 1, Averaged $[Ca^{2+}]$ transients in response to n sodium action potentials (arrows) evoked by current injection (n AP) measured at various heights above the soma (averages of 4–15 trials each). Interspike intervals within a burst were 6–8 ms. 2, Map of $[Ca^{2+}]$ transients along the apical dendrite. 3, Amplitudes of $[Ca^{2+}]$ transients evoked by two and three action potentials, normalized to transients evoked by one action potential.

pyramidal cells can produce calcium spikes *in vitro*. Furthermore, in the presence of the sodium channel blocker QX-314, layer 2/3 neurons produce calcium spikes in response to sensory activation²³, perhaps due to partial blockade of potassium currents⁴³. In some dendritic penetrations ($n = 6/15$), moderate current injections (~ 0.5 nA) evoked slow depolarizations and oscillations that resembled calcium spikes, as reported in brain slices^{10,15} (Fig. 5). These depolarizations were accompanied by very large $[Ca^{2+}]$ transients that decayed only slowly from their peak value. The slow membrane-potential time-course and large $[Ca^{2+}]$ transients together suggested that these events are calcium spikes. In the cases where regenerative calcium spikes could not be evoked (9/15 experiments), very large current injections (> 1 nA) could still produce large $[Ca^{2+}]$ transients (data not shown). Calcium-spike-evoked $[Ca^{2+}]$ transients were widespread, but decreased in amplitude towards the tips of dendrites ($n = 2$; data not shown). They could be observed in regions of the dendritic tree where bursts of sodium spikes did not produce significant calcium influx (Fig. 5a and 1). Thus the dendrites of layer 2/3 pyramidal cells can support calcium action potentials even *in vivo*, with pronounced background activity.

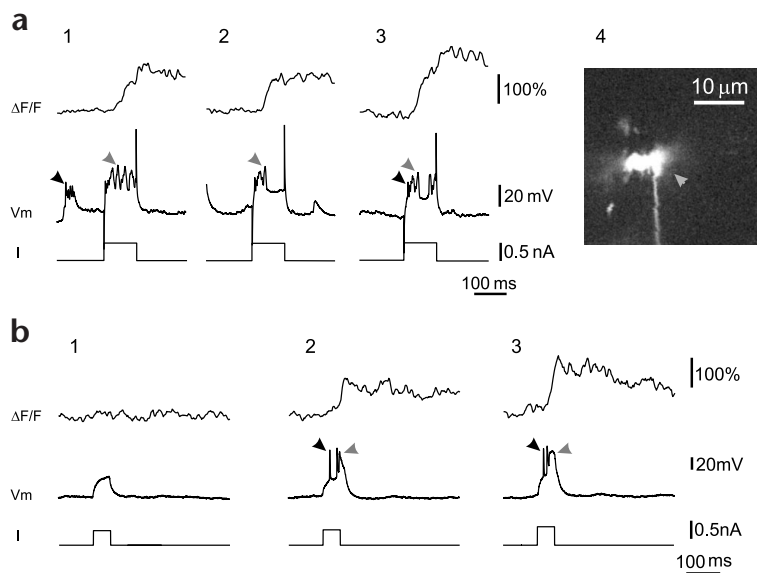
MODULATION OF DENDRITIC CALCIUM INFLUX BY TAIL PINCH
In urethane-anesthetized rats, tail pinch (~ 0.5 s) is a natural stimulus producing cortical activation mediated in part by nucleus basalis³¹, consistent with acetylcholine release³². The cellular correlates of tail pinch included desynchronization of the cortical EEG and transient membrane depolarization by ~ 2 –5 mV (Fig. 6a and c). Tail pinch typically increased the amplitude of

whisker-deflection-evoked $[Ca^{2+}]$ transients (Fig. 6a and b), but in some cases, $[Ca^{2+}]$ transient amplitudes were unchanged or even decreased. Tail pinch did not change the amplitude of dendritic sodium action potentials (ratio after and before tail pinch, 0.98 ± 0.3 , $n = 4$; Fig. 6c and d). Similarly, tail pinch did not enhance the calcium influx per action potential (ratio, 0.90 ± 0.14 , $n = 11$; Fig. 6e, f and g). Therefore, although tail pinch can enhance dendritic $[Ca^{2+}]$ transients evoked by sensory stimulation, the mechanism is enhanced spiking in response to sensory stimulation and not enhanced calcium influx per action potential (Fig. 6g). The average enhancement factor, defined as the ratio of action potential number or integral of the $[Ca^{2+}]$ transient, after and before tail pinch, was 1.8 ± 0.28 (mean \pm standard error, $n = 16$) Data were pooled from experiments including imaging and electrophysiology ($n = 11$), imaging alone ($n = 2$) or electrophysiology alone ($n = 3$).

Discussion

Dendritic calcium influx and the underlying electrogenesis are implicated in the induction of long-term synaptic plasticity^{6,7}, but *in vivo* studies are necessary to assess the importance of such cellular phenomena to system function. Previously we described the basic properties of dendritic $[Ca^{2+}]$ dynamics in layer 2/3 pyramidal neurons in barrel cortex *in vivo*²³. One finding of that study, that action potentials did not evoke $[Ca^{2+}]$ transients in distal dendrites, suggested that excitability in these dendrites is limited as compared to the dendrites of CA1 (refs 6, 41, 42) and layer 5 pyramidal cells^{2,38} in brain slices and CA1 pyramidal cells

Fig. 5. Dendritic Ca^{2+} spikes evoked by current injection. **(a)** Membrane potential recording in a distal apical dendrite ($\sim 150 \mu\text{m}$ from the soma; soma was $250 \mu\text{m}$ deep) and $[\text{Ca}^{2+}]$ measurement close to the recording electrode under ketamine anesthesia. Bursts of sodium action potentials (1, 3, black arrows) did not evoke dendritic $[\text{Ca}^{2+}]$ transients, whereas slow regenerative events (1, 2, 3, gray arrows) evoked by current injection ($\sim 0.5 \text{ nA}$) produced large $[\text{Ca}^{2+}]$ transients. 4, High-magnification image of the electrode penetration site. The micropipette penetrated a small secondary dendritic branch (arrow). Note the small swelling produced by the electrode and nearby dendritic spines. The apparent undulations in the image of the micropipette are due to heartbeat-associated movement. **(b)** Membrane potential recording in a proximal apical dendrite ($\sim 50 \mu\text{m}$ from the soma; cell was $370 \mu\text{m}$ deep) and $[\text{Ca}^{2+}]$ measurements $110 \mu\text{m}$ from the soma under urethane anesthesia. Subthreshold depolarizations (1) or Na^+ action potentials alone (2, 3, black arrows) evoke no or small Ca^{2+} influx, while slow regenerative potentials produced large $[\text{Ca}^{2+}]$ transients (2, 3, gray arrows).



*in vivo*²¹. The biophysical mechanism of this failure is important because it can shed light on the mechanisms of regulation of dendritic excitability and its relationship to synaptic plasticity in the intact brain. Because we did not measure the dendritic membrane potential in the previous study, several explanations could have accounted for that observation. For example, action potential propagation could be restricted *in vivo*, or VSCC density could be smaller in this region of the dendritic tree.

To resolve these questions, we recorded dendritic membrane potential with sharp electrodes together with 2PLSM imaging of $[\text{Ca}^{2+}]$ dynamics. Our main new findings are, first, that dendritic sodium action potentials attenuate rapidly with distance from the soma, consistent with passive spread of depolarizations into dendrites. Second, layer 2/3 dendrites can support calcium action potentials *in vivo* in response to direct current injection. Third, activation of neuromodulatory systems by tail pinch increases dendritic $[\text{Ca}^{2+}]$ transients evoked by whisker deflection because of a general increase in neuronal excitability, but not by boosting action potential backpropagation or calcium influx per action potential.

$[\text{Ca}^{2+}]$ TRANSIENTS EVOKED BY SODIUM ACTION POTENTIALS

The membrane potential of layer 2/3 pyramidal cells showed slow oscillations that were highly correlated with the EEG recording (Figs 1b, 2a, 3a and 6a and c). Similarly, whisker-evoked postsynaptic potentials were apparent in the EEG. These observations indicate that both background and sensory-evoked cortical activity may be highly synchronized. Consistent with our previous findings, dendritic $[\text{Ca}^{2+}]$ transients were typically associated with intracellularly recorded sodium action potentials (Figs 2a, c and d, 4 and 6), whether evoked by sensory stimulation, somatic current injection or spontaneous postsynaptic potentials. $[\text{Ca}^{2+}]$ rose rapidly (within $< 2 \text{ ms}$, the temporal resolution of our scanner) during sodium action potentials (Fig. 2a–c), presumably mediated by the opening of VSCCs³. Sodium action potentials produced by whisker deflection were smaller and shorter than those produced by current injections (Fig. 1c and d); they also produced smaller dendritic $[\text{Ca}^{2+}]$ transients (Fig. 2c), show-

ing that action potential shape is an important determinant of dendritic calcium influx. Amplitudes of $[\text{Ca}^{2+}]$ transients and action potentials in dendrites suggest that action-potential-evoked dendritic calcium influx is primarily due to high-voltage-activated VSCCs.

The amplitudes of $[\text{Ca}^{2+}]$ transients produced by somatic sodium action potentials were not uniform throughout the dendritic tree, but peaked in the proximal apical dendrite and then rapidly decreased with distance from the soma (Figs. 2d and 4). This suggests that action potentials radiate into dendrites in a decremental fashion, failing to open VSCCs farther out in the dendrites.

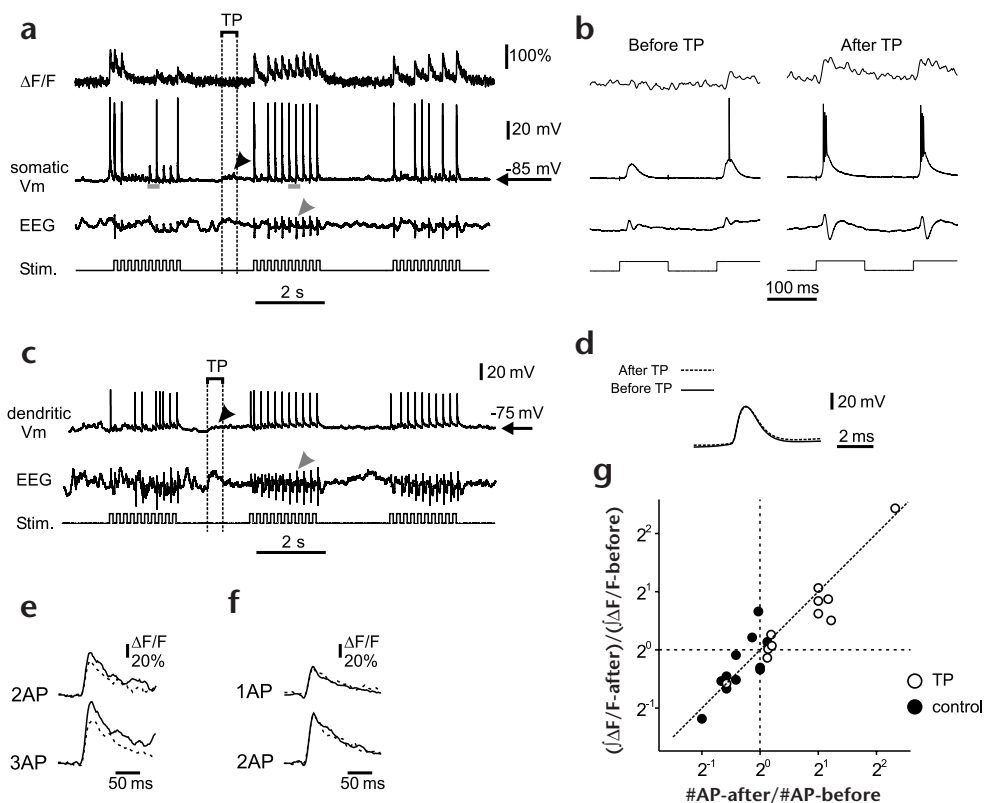
DENDRITIC SODIUM ACTION POTENTIALS

The amplitude of sodium action potentials decreased rapidly with distance from the soma. This rate of decrement is consistent with predictions from simulations of passive action potential spread^{39,40}. In these models, and in our experiments, the action potential amplitude decays to one-half the somatic amplitude $\sim 100 \mu\text{m}$ from the soma (Fig. 3c).

Another finding consistent with failure of backpropagation is that fluorescence transients produced by bursts of action potentials scale approximately linearly with action potential number (Fig. 4). Occasionally a slight supralinearity could even be detected. Because the large $[\text{Ca}^{2+}]$ transients ($\Delta F/F > 400\%$) observed almost certainly pushed the indicator close to saturation, $[\text{Ca}^{2+}]$ supralinearities were probably larger than they appear from fluorescence nonlinearities. In contrast, activity-dependent failure of sodium action-potential backpropagation, as observed in CA1 pyramidal neurons *in vivo*, would predict a sublinear dependence of $[\text{Ca}^{2+}]$ transient amplitude on action potential number. Our findings are consistent with failure of backpropagation for even the first action potential in a burst. Several mechanisms could underlie this failure of dendritic excitability, including shunting by inhibitory^{13,14,20} or excitatory^{19,21} synaptic activity, chronic inactivation of sodium conductances^{17,18}, other changes in dendritic channel properties¹⁶ or activity of modulatory systems^{12,26}.

Action-potential-evoked $[\text{Ca}^{2+}]$ transients from deeper cells

Fig. 6. Modulation of dendritic $[Ca^{2+}]$ transients by tail pinch. **(a)** Tail pinch (TP, between vertical dashed lines) enhances average $[Ca^{2+}]$ transient amplitude ($\Delta F/F$) in response to whisker stimulation. Tail pinch produced a slight depolarization in the membrane potential (V_m , black arrowhead) and increased reliability in the spiking response to whisker deflection. Similarly, tail pinch increased reliability in the whisker response in the EEG potential (EEG, grey arrowhead). The effects of tail pinch lasted 5–50 s. The soma was 280 μm deep; measurements were taken 72 μm above the soma. **(b)** Enlargement of segments before and after tail pinch (indicated by gray bars under the V_m trace in a). After tail pinch, whisker stimuli produced a larger burst of action potentials than before tail pinch, producing larger $[Ca^{2+}]$ transients. **(c)** Effect of tail pinch on sodium action potential size in the dendrites. Membrane potential measurement was $> 50 \mu m$ above the soma. **(d)** Averaged action potential amplitude and shape before (solid line) and after (dashed line) tail pinch (same cell as c). **(e)** $[Ca^{2+}]$ transients associated with two (2AP) and three (3AP) action potentials before (solid line) and after (dashed line) tail pinch (same experiment as in a, b; averages of 3–5 trials, low-pass filtered). Note that the calcium influx per action potential actually decreased after tail pinch. **(f)** $[Ca^{2+}]$ transients associated with one (1AP) and two (2AP) action potentials before (solid line) and after (dashed line) tail pinch (different neuron; averages of 10 trials, low-pass filtered). Note that the calcium influx per action potential is unchanged. **(g)** Summary of tail-pinch data. Responses to whisker stimulus trains before and immediately after tail pinch were compared. Ratio of integrals of $[Ca^{2+}]$ transient amplitudes, $(\int \Delta F/F\text{-after})/(\int \Delta F/F\text{-before})$, and the ratio of action potential numbers ($\#AP\text{-after}/\#AP\text{-before}$) plotted against each other (open circles). Also plotted are ratios derived from whisker-stimulus trains without intervening tail pinch (control, solid circles). Note that the control data show some adaptation, whereas tail pinch produces potentiation. Most points lie close to the diagonal line, indicating that $[Ca^{2+}]$ transient amplitudes per action potential remained constant.



attenuate more gradually than those recorded from more superficial cells (Fig. 2d), perhaps because dendrites of deeper cells tend to be thicker, producing less serial resistance and thus less decrement with distance of the action-potential amplitude. One possible interpretation of this finding is that dendritic action potentials are generally limited to layers 2 and 3 and are excluded from the tuft branches of layer 1.

DENDRITIC CALCIUM SPIKES

Here, as before²³, we were unable to evoke dendritic calcium action potentials by sensory stimulation in layer 2/3 pyramidal neurons, but we found that layer 2/3 dendrites can generate calcium spikes in response to large current injections (Fig. 5). Our sensory stimulation protocol may not be appropriate to evoke calcium spikes *in vivo*. Perhaps behaviorally relevant stimuli during arousal evoke calcium spikes, as a trigger for synaptic plasticity.

2PLSM was crucial to identifying calcium spikes; membrane potential measurements alone would have been insufficient. For example, dendritic PSPs can resemble calcium spikes in shape

but may not be associated with massive calcium influx (Fig. 5a and 1). In contrast, current-injection-evoked calcium spikes were associated with large calcium influx (Fig. 5).

Perhaps sodium action-potential backpropagation and/or dendritic calcium spikes require specific patterns of synaptic activity, possibly associated with particular behavioral states. One concern is that our results could have been perturbed by the anesthetic. Addressing this issue will ultimately require measuring cellular physiology in behaving animals. However, the spread of dendritic excitation in our preparation is similar with either ketamine or urethane, anesthetics that produce different EEG patterns and presumably have different pharmacological profiles. For example, ketamine, but not most other anesthetics, makes sensory-stimulation-evoked potentials larger than during waking⁴⁹, suggesting that our results are not due to specific pharmacological effects. In addition, preliminary data show that layer 5 cells produce sensory-stimulation-evoked calcium spikes and large fast spikes in distal dendrites (unpublished observations; F.H., K.S., W.D. & D.W.T. *Soc. Neurosci. Abstr.*, 37.6, 1998), demonstrating that the failure of excitability observed in the

dendrites of layer 2/3 neurons is not a general anesthesia effect. Rather it seems that dendritic excitability is highly regulated and functionally diverse.

EFFECTS OF ACTIVATING SYSTEMS

Various subcortical neuromodulatory centers innervate the neocortex. Activity in these structures is correlated with behavioral states²⁸. Neuromodulators can profoundly affect cellular membrane properties. For example, muscarinic agonists increase dendritic excitability in CA1 pyramidal cells in brain slices^{12,26}. Stimulation of cholinergic centers *in vivo* increases sensitivity to sensory stimuli and can drastically reduce the threshold for LTP induction⁴⁵ and receptive field plasticity⁴⁶. We hypothesized that cholinergic and perhaps other modulatory systems⁴⁷ could control dendritic excitability in the intact brain. Therefore we studied the effects of tail pinch on dendritic $[Ca^{2+}]$ dynamics. Tail pinch activates nucleus basalis³¹ and other neuromodulatory systems, consistent with increasing acetylcholine levels in neocortex³². Tail pinch desynchronized the EEG (low-voltage, fast activity) and slightly depolarized the membrane potential (Fig. 6a and c). These effects were similar to those reported for nucleus basalis stimulation⁴⁴.

Tail pinch most often increased the dendritic calcium influx in response to a train of whisker stimuli, because it caused these stimuli to produce more action potentials on average (Fig. 6a, b and g). Dendritic $[Ca^{2+}]$ transient amplitudes for a fixed number of action potentials did not increase with tail pinch (Fig. 6e and g). Consistent with this finding, the amplitudes of dendritically recorded sodium action potentials did not change (Fig. 6c and d). This shows that although tail pinch changed dendritic excitation in response to a stimulus, this effect was not due to changes in backpropagation. The enhancement of stimulus-evoked dendritic $[Ca^{2+}]$ following tail pinch could explain the lowered threshold for LTP induction in response to afferent stimulation following tail pinch⁴⁸. This cellular mechanism could also underlie the neocortical map reorganization enabled by activation of nucleus basalis^{45,46}.

Methods

IN VIVO ELECTROPHYSIOLOGY. Sprague-Dawley rats (age 5–8 weeks, $n = 35$; Fisher retired breeders, $n = 15$; WAG/Ris, 300–400 grams, $n = 10$) were anesthetized with urethane (1.5 mg per g body weight, $n = 40$). Other experiments used a mixture of ketamine (25 mg/ml), xylazine (1.25 mg/ml) and acepromazine (.25 mg/ml; 2.7 ml per kg body weight, $n = 20$), which gave similar results, except that tail pinch had no effect under these conditions. The skull over barrel cortex was thinned until major blood vessels could be seen. A small craniotomy (2–3 mm on the side) was then opened above an area devoid of major vessels, and the dura was carefully removed. The exposed area was covered with agarose (1.5–2%, Type III-A, Sigma) in artificial cerebral spinal fluid consisting of 125 mM NaCl, 5 mM KCl, 10 mM glucose, 10 mM HEPES, 2 mM $CaCl_2$ and 2 mM $MgCl_2$, pH 7.4. The agarose was covered by a number-1 coverslide mounted on a stainless-steel frame, which was then secured to the skull with dental cement and fixed to the microscope stage. Sharp recording electrodes were filled with 400 mM potassium acetate buffered with 1 mM HEPES at pH 7.4, containing 3–6 mM Calcium Green 1 or Oregon Green Bapta 1 (Molecular Probes). In some experiments, 2% neurobiotin (Vector Labs) was also included. Microelectrodes were beveled to resistances from 50–100 M Ω . Membrane potential recordings were made with an intracellular amplifier (Neurodata IR283) and stored digitally. Neurons with resting membrane potentials more negative than –60 mV were iontophoretically filled with indicator dye by injecting hyperpolarizing current (–0.2 nA to –0.5 nA, 5 min). During filling, one to three whiskers were deflected (5–10 degrees) in a sequence of ten square deflections at 5 Hz using a pencil lead attached to a galvanometer

scanner. Different whiskers were probed until a reliable response was evoked. Input resistances, estimated by using the bridge balance to compensate for voltage transients produced by 0.2-nA current pulses, were 20–100 M Ω . To stimulate cortical activating systems³¹, the base of the rat's tail was pinched with forceps for 0.5–1 s.

For epidural field potential recordings (EEG), a small hole was drilled into the skull just lateral to the craniotomy. A teflon-coated silver wire (diameter 125 μ m) was slid under the skull and fixed into place with dental cement. An epidural reference electrode was placed above cerebellum. The differential signal was amplified ($\times 1000$), bandpass filtered (0.1–300 Hz) and stored digitally.

IN VIVO TWO-PHOTON IMAGING. Imaging was done with a custom microscope. The light source for two-photon excitation was a pulsed Ti:sapphire laser (Tsunami, Spectra Physics) operating at 80 MHz repetition frequency, 100 fs pulse width, and wavelength in the range 800–850 nm. Excitation light was focused by a 40 \times immersion objective (0.75 NA, Carl Zeiss). The average power delivered to the brain was < 200 mW. Scanning used two galvanometer mirrors (Cambridge Technology, model 6800). Scanning and image acquisition were controlled with custom software (R. Stepnoski, Lucent Technologies). Emitted light was collected in epifluorescence mode and detected with a photomultiplier tube (Hamamatsu R9638). Sometimes parts of the dendritic tree were obscured by blood vessels, making it impossible to accurately determine the dendritic length between soma and electrode penetration. We therefore used the focal distance between soma and dendritic penetration as a measure of dendritic distance (Figs 2, 3 and 4). Actual dendritic lengths are estimated to be ~ 25% longer. Acquisition of images and electrophysiology were synchronized to 125 μ s. Fast fluorescence measurements were made by repeatedly scanning a single line across the dendrite at 2-ms time intervals. The resulting linescan image was used for quantitative analysis as follows: the fluorescence signal, F , was computed as an average along the scan line over the width of the dendrite; the baseline signal, F_{base} , was computed as an average over the same width for 3–10 scan lines before an event; the normalized change in fluorescence was then $\Delta F/F = (F - F_{base})/(F_{base} - B)$, where B is the background signal determined from averages on areas adjacent to the dendrite. At time scales longer than 1 ms, and apart from dye saturation, $\Delta F/F$ is proportional to $\Delta[Ca^{2+}]$. In Figs 2a and b and 5a, fluorescence traces were filtered for presentation using the Savitzky–Golay algorithm.

Could gradients in $[Ca^{2+}]$ indicator concentration have skewed the spatial maps of $[Ca^{2+}]$ transients? Dye gradients occur because the electrode is a point source of high concentrations (3–6 mM) of $[Ca^{2+}]$ indicator. At concentrations where the capacity of the added buffer begins to compete with the endogenous buffer (typically ~ 50 μ M of Bapta-based indicator), $[Ca^{2+}]$ transient amplitudes will decrease with increasing dye concentrations. In addition to its effect on $[Ca^{2+}]$ transient amplitude, large concentrations of $[Ca^{2+}]$ indicator lengthen the decay times of action-potential-evoked $[Ca^{2+}]$ transients (beyond ~ 100 ms); this makes dye gradients easy to detect. Because $[Ca^{2+}]$ transients were rapid (< 100 ms) in most cases (Figs 2a and b, 5 and 6), $[Ca^{2+}]$ indicator concentrations were probably sufficiently low not to perturb our results²⁵. However, long decay times were sometimes observed close to the recording electrode (Figs 2c and 3), indicating a relatively high concentration of $[Ca^{2+}]$ indicator and presumably depressed $[Ca^{2+}]$ transient amplitudes. In these cases, we might be underestimating amplitudes close to the electrode penetration relative to transients farther out in the dendrite. This of course does not change the finding that $[Ca^{2+}]$ transients evoked by sodium action potentials are absent in the distal dendrites. In some cases (for example Fig. 4b), fluorescence transients were larger (> 400%) than the largest transients observed in brain slices⁵ using the same indicator, suggesting that either the K_d of the indicator is higher at physiological temperatures or that the resting $[Ca^{2+}]$ is lower *in vivo*. Data were analyzed using the IDL programming language (Research Systems Inc.).

HISTOLOGICAL PREPARATIONS. At the end of some experiments, animals were perfused intracardially with cold saline (60 ml, PBS) followed by 60 ml of fixative (4% paraformaldehyde in 0.1 M PBS). Barrel cortex was dissected out and stored in 4% paraformaldehyde overnight and then transferred to 30% sucrose for at least 24 hours (all in 0.1 PBS). The brain

was sectioned on a cryomicrotome (thickness, 60 μm). Sections were incubated in avidin-biotin-peroxidase complex solution (ABC elite kit, Vector Labs) and processed for intracellular peroxidase staining⁵⁰.

Acknowledgements

We thank G. Buzsaki for suggestions, B. Burbach for help with histology, and G. Major, Z. Mainen and E. Stern for comments on the manuscript. This work was supported by Lucent Technologies and the Klingenstein, Pew, and Whitaker Foundations (K.S.), and the Max-Planck Society (F.H.).

RECEIVED 27 AUGUST; ACCEPTED 17 NOVEMBER 1998

- Stuart, G. J. & Sakmann, B. Active propagation of somatic action potentials into neocortical pyramidal cell dendrites. *Nature* 367, 69–72 (1994).
- Yuste, R. & Tank, D. W. Dendritic integration in mammalian neurons, a century after Cajal. *Neuron* 16, 701–716 (1996).
- Jaffe, D. B. *et al.* The spread of Na^+ spikes determines the pattern of dendritic Ca^{2+} entry into hippocampal neurons. *Nature* 357, 244–246 (1992).
- Magee, J. C. & Johnston, D. Synaptic activation of voltage-gated channels in the dendrites of hippocampal pyramidal neurons. *Science* 268, 301–304 (1995).
- Yuste, R. & Denk, W. Dendritic spines as basic functional units of neuronal integration. *Nature* 375, 682–684 (1995).
- Magee, J. C. & Johnston, D. A synaptically controlled, associative signal for Hebbian synaptic plasticity in hippocampal neurons. *Science* 275, 209–213 (1997).
- Markram, H., Lübke, J., Frotscher, M. & Sakmann, B. Regulation of synaptic efficacy by coincidence of postsynaptic APs and EPSPs. *Science* 275, 213–215 (1997).
- Turner, R. W., Meyers, E. R., Richardson, D. L. & Barker, J. L. The site of initiation of action potential discharge over the somatosensory axis of rat hippocampal CA1 neurons. *J. Neurosci.* 11, 2270–2280 (1991).
- Cauller, L. J. & Connors, B. W. in *Single Neuron Computation* (eds McKenna, T., Davis, J. & Zornetzer, S. F.) 199–229 (Academic, New York, 1992).
- Kim, H. G. & Connors, B. W. Apical dendrites of the neocortex: correlation between sodium- and calcium-dependent spiking and pyramidal cell morphology. *J. Neurosci.* 13, 5301–5311 (1993).
- Schiller, J., Schiller, Y., Stuart, G. & Sakmann, B. Calcium action-potentials restricted to distal apical dendrites of rat neocortical pyramidal neurons. *J. Physiol. (Lond.)* 505, 605–616 (1997).
- Tsubokawa, H. & Ross, W. N. Muscarinic modulation of spike backpropagation in the apical dendrites of hippocampal CA1 pyramidal neurons. *J. Neurosci.* 17, 5782–5791 (1997).
- Tsubokawa, H. & Ross, W. N. IPSPs modulate spike backpropagation and associated $[\text{Ca}^{2+}]$ changes in the dendrites of hippocampal CA1 pyramidal neurons. *J. Neurophysiol.* 76, 2896–2906 (1996).
- Kim, H. G., Beierlein, M. & Connors, B. W. Inhibitory control of excitable dendrites in neocortex. *J. Neurophysiol.* 74, 1810–1814 (1995).
- Andreasen, M. & Lambert, J. D. C. Regenerative properties of pyramidal cell dendrites in area CA1 of the rat hippocampus. *J. Physiol. (Lond.)* 483, 421–441 (1995).
- Hoffman, D. A., Magee, J. C., Colbert, C. M. & Johnston, D. K^+ channel regulation of signal propagation in dendrites of hippocampal pyramidal neurons. *Nature* 287, 869–875 (1997).
- Jung, H. Y., Mickus, T. & Spruston, N. Prolonged sodium channel inactivation contributes to dendritic action potential attenuation in hippocampal pyramidal neurons. *J. Neurosci.* 17, 6639–6646 (1997).
- Colbert, C. M., Magee, J. C., Hoffman, D. A. & Johnston, D. Slow recovery from inactivation of Na^+ channels underlies activity-dependent attenuation of dendritic action potentials in hippocampal CA1 pyramidal neurons. *J. Neurophysiol.* 17, 6512–6521 (1997).
- Pare, D., Shink, E., Gaudreau, H., Destexhe, A. & Lang, E. J. Impact of spontaneous synaptic activity on the resting properties of cat neocortical pyramidal neurons *in vivo*. *J. Neurophysiol.* 79, 1450–1460 (1998).
- Pare, D., Lang, E. J. & Destexhe, A. Inhibitory control of somatodendritic interactions underlying action potentials in neocortical pyramidal neurons *in vivo*: an intracellular and computational study. *Neuroscience* 84, 377–402 (1998).
- Kamondi, A., Acsády, L. & Buzsáki, G. Dendritic spikes are enhanced by cooperative network activity in the intact hippocampus. *J. Neurosci.* 18, 3919–3928 (1998).
- Denk, W., Strickler, J. H. & Webb, W. W. Two-photon laser scanning microscopy. *Science* 248, 73–76 (1990).
- Svoboda, K., Denk, W., Kleinfeld, D. & Tank, D. W. *In vivo* dendritic calcium dynamics in neocortical pyramidal neurons. *Nature* 385, 161–165 (1997).
- Denk, W. & Svoboda, K. Photon upmanship: why multiphoton imaging is more than a gimmick. *Neuron* 18, 351–357 (1997).
- Helmchen, F., Imoto, K. & Sakmann, B. Ca^{2+} buffering and action potential-evoked Ca^{2+} signaling in dendrites of pyramidal neurons. *Biophys. J.* 70, 1069–1081 (1996).
- Muller, W. & Connor, J. A. Cholinergic input uncouples Ca^{2+} changes from K^+ conductance activation and amplifies intradendritic Ca^{2+} changes in hippocampal neurons. *Neuron* 6, 901–905 (1991).
- Juliano, S. L. & Jacobs, S. E. in *The Barrel Cortex of Rodents* (eds Jones, E. G. & Diamond, I. T.) 411–430 (Plenum, New York, 1995).
- Buzsáki, G. *et al.* Nucleus basalis and thalamic control of neocortical activity in the freely moving rat. *J. Neurosci.* 8, 4007–4026 (1988).
- Winkler, J., Suhr, S., Gage, F., Thal, L. & Fisher, L. Essential role of neocortical acetylcholine in spatial memory. *Nature* 375, 484–487 (1995).
- Moruzzi, G. & Magoun, H. W. Brainstem reticular formation and activation of the EEG. *Electroencephalogr. Clin. Neurophysiol.* 1, 455–473 (1949).
- Detari, L. & Vanderwolf, C. H. Activity of identified cortically projecting and other basal forebrain neurones during large slow waves and cortical activation in anesthetized rats. *Brain Res.* 437, 1–8 (1987).
- Mullin, W. J. The effect of graded forelimb afferent volleys on acetylcholine release from cat sensorimotor cortex. *J. Physiol. (Lond.)* 244, 741–756 (1975).
- Connors, B. W. & Gutnick, M. J. Intrinsic firing patterns of diverse neocortical neurons. *Trends Neurosci.* 13, 99–104 (1990).
- Cowan, R. L. & Wilson, C. J. Spontaneous firing pattern and axonal projections of single corticostriatal neurons in the rat medial agranular cortex. *J. Neurophysiol.* 71, 17–32 (1994).
- Contreras, D. & Steriade, M. Synchronization of low frequency rhythms in corticothalamic networks. *Neuroscience* 76, 11–24 (1997).
- Crevier, D. W. & Meister, M. Synchronous period-doubling in flicker vision of salamander and man. *J. Neurophysiol.* 79, 1869–1878 (1998).
- White, E. L. *Cortical Circuits* (Birkhauser, Boston, 1989).
- Stuart, G., Schiller, J. & Sakmann, B. Action potential initiation and propagation in rat neocortical pyramidal neurons. *J. Physiol. (Lond.)* 505, 617–632 (1997).
- Rapp, M., Yarom, Y. & Segev, I. Modeling back propagating action potential in weakly excitable dendrites of neocortical pyramidal cells. *Proc. Natl. Acad. Sci. USA* 93, 11985–11990 (1996).
- Mainen, Z. F., Joerges, J., Huguenard, J. R. & Sejnowski, T. J. A model of spike initiation in neocortical pyramidal neurons. *Neuron* 15, 1427–1439 (1995).
- Callaway, J. C. & Ross, W. N. Frequency-dependent propagation of sodium action potentials in dendrites of hippocampal CA1 pyramidal neurons. *J. Neurophysiol.* 74, 1395–1403 (1995).
- Spruston, N., Schiller, Y., Stuart, G. & Sakmann, B. Activity-dependent action potential invasion and calcium influx into hippocampal CA1 dendrites. *Science* 268, 297–300 (1995).
- Andreasen, M. & Hablitz, J. J. Local anesthetics block transient outward potassium currents in rat neocortical neurons. *J. Neurophysiol.* 69, 1966–1975 (1993).
- Metherate, R., Cox, C. L. & Ashe, J. H. Cellular basis of neocortical activation: modulation of neural oscillations by the nucleus basalis and endogenous acetylcholine. *J. Neurosci.* 12, 4701–4711 (1992).
- Bakin, J. S. & Weinberger, N. M. Induction of a physiological memory in the cerebral cortex by stimulation of the nucleus basalis. *Proc. Natl. Acad. Sci. USA* 93, 11219–11224 (1996).
- Kilgard, M. P. & Merzenich, M. M. Cortical map organization enabled by nucleus basalis activity. *Science* 279, 1714–1718 (1998).
- McCormick, D. A. Neurotransmitter actions in the thalamus and cerebral cortex and their role in neuromodulation of thalamocortical activity. *Progr. Neurobiol.* 29, 337–388 (1992).
- Holscher, C., Anwyl, R. & Rowan, M. J. Stimulation on the positive phase of hippocampal theta rhythm induces long-term potentiation that can be depotentiated by stimulation on the negative phase in area CA1 *in vivo*. *J. Neurosci.* 17, 6470–6477 (1997).
- Sloan, T. B. Anesthetic effects on electrophysiologic recordings. *J. Clin. Neurophysiol.* 15, 217–226 (1998).
- Horikawa, K. & Armstrong, W. E. A versatile means of intracellular labeling: injection of biocytin and its detection with avidin conjugates. *J. Neurosci. Methods* 25, 1–11 (1988).